SETAC PRESS

Environmental Toxicology and Chemistry, Vol. 23, No. 10, pp. 2441–2456, 2004

Printed in the USA
0730-7268/04 $12.00 + .00

Special Issue Honoring Don Mackay

OIL SPILL IMPACT MODELING: DEVELOPMENT AND VALIDATION

DEBORAH P. FRENCH-MCCAY
Applied Science Associates, Narragansett, Rhode Island 02882, USA

(*Received* 10 *July* 2003; *Accepted* 23 *December* 2003)

Abstract—A coupled oil fate and effects model has been developed for the estimation of impacts to habitats, wildlife, and aquatic organisms resulting from acute exposure to spilled oil. The physical fates model estimates the distribution of oil (as mass and concentrations) on the water surface, on shorelines, in the water column, and in the sediments, accounting for spreading, evaporation, transport, dispersion, emulsification, entrainment, dissolution, volatilization, partitioning, sedimentation, and degradation. The biological effects model estimates exposure of biota of various behavior types to floating oil and subsurface contamination, resulting percent mortality, and sublethal effects on production (somatic growth). Impacts are summarized as areas or volumes affected, percent of populations lost, and production foregone because of a spill's effects. This paper summarizes existing information and data used to develop the model, model algorithms and assumptions, validation studies, and research needs. Simulation of the *Exxon Valdez* oil spill is presented as a case study and validation of the model.

Keywords—Oil spill Model Fates/effects Impact *Exxon Valdez*

INTRODUCTION

A large number of oil spill models have been developed over the past 30 years, and several comprehensive reviews of oil spill trajectory and fate modeling have been performed [1–5] to assess the state of the practice, summarize key developments, and project future research. The vast majority of oil spill models (the focus of these reviews) are used to predict or hindcast the trajectory [6–10], weathering [11–14], and fate [12,15–28] of oil spilled on or near the surface of water, with the purposes of informing spill response (real time or in drills), performing contingency planning, and evaluating the behavior and mass balance. Relatively few models have been designed and used to quantitatively evaluate the impacts of oil on aquatic organisms and habitats (as described below). This paper describes such a model, which represents the state-of-the-art of coupled oil fate and effects model systems. The Spill Impact Model Application Package (SIMAP) was derived from the physical fates and biological effects submodels in the Natural Resource Damage Assessment Model for Coastal and Marine Environments, which were developed for the U.S. Department of the Interior as the basis of Comprehensive Environmental Response, Compensation, and Liability Act of 1980, and the Natural Resource Damage Assessment (NRDA) regulations for Type A assessments [29,30]. The technical development involved several in-depth peer reviews, as described in the Final Rule [29]. The Spill Impact Model Application Package has been developed further for use in impact and ecological risk, as well as natural resource damage assessment. The physical fates model draws on research and model development in common with the larger universe of trajectory and oil fate models. The biological effects model includes innovative algorithms to quantify the impact of oil on biological resources: Habitats, aquatic organisms (fish, invertebrates, aquatic plants, plankton), and wildlife (birds, mammals, reptiles).

The reader is referred to the above reviews for discussion of oil trajectory and fate model development. Earlier modeling efforts for impact assessment relied on calculating the intersection of oil trajectories with biota, assuming an impact threshold [31–38]. In some cases, wildlife (seabird or marine mammal) population and migration models were used to simulate the distribution, behavior, and recovery of the affected species, in conjunction with their intersection with oil trajectories [39–45]. In these modeling efforts, the impact threshold for wildlife appropriately was based on an oil thickness or mass for lethal or sublethal effects, although quantitative information definitively indicating what dose would be lethal was not available.

However, for aquatic organisms, impact thresholds based on surface oil are inadequate, particularly when evaluating the change in impact caused by use of chemical dispersants on spills. Mackay and Leinonen [16] and Mackay et al. [17,18] suggested that meaningful assessments of impacts on aquatic biota can be accomplished only after quantitative understanding of the natural and chemical dispersion processes (entrainment), as the major toxic effect of oil is from dissolved hydrocarbons, and the main dissolution mechanism is via dispersed oil droplets rather than surface slicks. Based on theoretical calculations and modeling results, Mackay and Leinonen [16] showed that: Dissolution from surface slicks is insignificant and can be neglected safely and dissolution time from subsurface droplets less than 100 μm in diameter has a half-life of less than 13 min. The dissolution rate is very sensitive to the droplet size (because it involves mass transfer across the surface area of the droplet), and the amount of hydrocarbon mass dissolved is a function of the mass entrained and droplet size distribution. In turn, these are a function of soluble hydrocarbon content of the oil, the amount of evaporation of these components before entrainment, oil viscosity (which increases as the oil weathers and emulsifies), oil surface tension (which may be reduced by surfactant dispersants), and the energy in the system (the higher the energy the smaller the droplets). Large droplets (greater than a few hundred microns in diameter) resurface rapidly, and so dissolution from those also is inconsequential.

* dfrench@appsci.com.

Table 1. Definition of four distillation cuts and the eight pseudo-components in the model (monoaromatic hydrocarbons, MAHs; benzene + toluene + ethylbenzene + xylene, BTEX; polynuclear aromatic hydrocarbons, PAHs)

Characteristic	Volatile and highly soluble	Semivolatile and soluble	Low volatility and slightly soluble	Residual (nonvolatile and insoluble)
Distillation cut	1	2	3	4
Boiling point (°C)	<180	180–265	265–380	>380
Molecular weight	50–125	125–168	152–215	>215
Log(K_{OW})	2.1–3.7	3.7–4.4	3.9–5.6	>5.6
Aliphatic pseudo-components: No. of carbons	Volatile aliphatics: C4–C10	Semivolatile aliphatics: C10–C15	Low-volatility aliphatics: C15–C20	Nonvolatile aliphatics: >C20
Aromatic pseudo-component name: Included compounds	MAHs: BTEX, MAHs to C3-benzenes	2-ring PAHs: C4-benzenes, 2-ring to C2-naphthalenes	3-ring PAHs: C3-, C4-naphthalenes, 3- to 4-ring PAHs with log(K_{OW}) < 5.6	≥4-ring aromatics: PAHs with log(K_{OW}) > 5.6 (insoluble)

Thus, both subsurface oil droplets and dissolved hydrocarbons explicitly must be simulated (in addition to surface-floating oil and associated processes) in an oil fates model to evaluate exposure of aquatic biota to oil hydrocarbons and biological effects. A prime example is the *North Cape* oil spill of January 1996, which occurred during a severe winter storm [46]. The barge *North Cape* spilled 828,000 gallons (2,682 metric tons) of home heating oil (No. 2 fuel oil) into the surf zone on the south coast of Rhode Island, USA. Most of the oil was entrained into the water column by heavy surf, resulting in high concentrations of dissolved components in shallow water that killed millions of water column and benthic organisms [46]. Though models based on surface oiling may be useful in predicting the trajectory of slicks and impacts on wildlife and shorelines, they cannot evaluate the extent of impacts to aquatic biota caused by subsurface oil.

Moreover, because the many hydrocarbons in oil have varying physical–chemical properties (most significantly those related to solubility and volatility), the oil fates model must separately track chemical classes or pseudocomponents of the whole oil with characteristics typical of the chemical group to simulate their separate fates [21,28,30,47–49]. Most oil fates models (including SIMAP) employ a Lagrangian particle approach, which enables the modeler to track physical and chemical property changes as oil weathers, which is particularly needed when oil is released over time under varying conditions [4]. This solution methodology also is used in SIMAP to track organisms' movements and exposure to the bioavailable components, those that are soluble or semisoluble.

Potential and documented impacts of oil in aquatic environments have been reviewed by the National Research Council [50,51] as well as others [30,52–54]. A biological effects model that considers all impacts would include evaluation of exposure considering movements and amounts of both oil and biota; acute effects algorithms for direct impacts (lethal and sublethal) in the short-term; consideration of sublethal effects of chronic contamination; indirect effects via reduction in food supply or habitat, or other changes in the ecosystem; behavioral changes resulting in reduced growth, survival, or reproductive success; impacts of response activities; and population level impacts caused by mortality and sublethal effects. Supporting research and information is available to quantify some but not all of these effects, as described below.

Finally, the oil fate model, as well as the biological effects model for planktonic organisms, should be driven by an accurate description of the winds and currents at all significant spatial and temporal scales in order to judge the performance of the oil fates and effects models. Wind data generally are available for most locations and times of interest. Typically, the most reliable and representative current data are those generated by a calibrated hydrodynamic model, unless site- and event-specific current measurements are available.

This paper summarizes existing information and the current state-of-the-art in oil fates and effects modeling, model algorithms and assumptions used in SIMAP, validation studies, and research needs. Simulation of the *Exxon Valdez* oil spill is presented as a case study and validation of the wildlife impact model. Validation and sensitivity studies indicate the main sources of uncertainty, data requirements for an accurate simulation, and research needs to improve our understanding and quantification of oil spill effects.

PHYSICAL FATES MODEL

The three-dimensional physical fates model estimates distribution (as mass and concentrations) of whole oil and oil pseudocomponents (i.e., fractions of the oil treated as a single chemical with properties representative of the included chemicals) on the water surface, on shorelines, in the water column, and in sediments. Oil fate processes included are spreading (gravitational and by shearing), evaporation from slicks, transport, randomized dispersion, emulsification, entrainment (natural and facilitated by dispersant), dissolution, volatilization of dissolved hydrocarbons from the surface water, adherence of oil droplets to suspended sediments, adsorption of soluble and semisoluble aromatics to suspended sediments, sedimentation, and degradation. Oil mass is tracked separately for lower molecular weight aromatics (1–3-ring aromatics), which cause toxicity [50–62], other volatiles, and nonvolatiles. The lower molecular weight aromatics dissolve from the whole oil and are partitioned in the water column and sediments according to equilibrium partitioning theory.

In the model, the oil is treated as eight pseudocomponents, characterized by volatility (boiling point), hydrophobicity (octanol–water partition coefficient, K_{ow}), and being aromatic or not (i.e., aliphatic): Volatile aliphatics, semivolatile aliphatics, aliphatics of low volatility, nonvolatile aliphatics (i.e., in the residual oil), volatile aromatics (monoaromatic hydrocarbons, [MAHs]), semivolatile aromatics (2-ring polynuclear aromatic hydrocarbons, [PAHs]), aromatics of low volatility (3-ring PAHs), and nonvolatile aromatics (in the residual; Table 1). Six of the components (all but the two nonvolatile residual components) evaporate at rates specific to the pseudocomponent. Solubility is correlated strongly with volatility, and the solubility of aromatics is higher than aliphatics of the same volatility, with the MAHs the most soluble, the 2-ring PAHs semisoluble, and the 3-ring PAHs slightly soluble [63–66].

Table 2. Physical–chemical properties for monoaromatic hydrocarbons. Molecular weight (MW), boiling point (BP), solubility, vapor pressure, and log(K_{OW}) are from Mackay et al. [63]

Compound(s)	Rings	Cs	MW (g/mol)	Distillation cut no.	BP (°C)	Solubility (ppm)	Vapor pressure (atm)	Log(K_{OW})
Benzene	1	6	78	1	80	1780	0.12534	2.1
Toluene	1	7	92	1	111	515	0.03750	2.7
Ethylbenzene	1	8	106	1	136	152	0.01253	3.1
o-Xylene	1	8	106	1	144	220	0.01155	3.2
p-Xylene	1	8	106	1	138	215	0.01155	3.2
m-Xylene	1	8	106	1	139	160	0.01086	3.2
Xylenes (mixture)	1	8	106	1	140	198	0.01132	3.2
Styrene	1	8	104	1	145	300	0.00868	3.1
Methylstyrenes	1	9	118	1	170	100	0.00264	3.4
1,2,3-Trimethylbenzene	1	9	120	1	176	70	0.00197	3.6
1,2,4-Trimethylbenzene (pseudocumene)	1	9	120	1	169	57	0.00266	3.6
1,3,4-Trimethylbenzene	1	9	120	1	169	57	0.00266	3.6
1,3,5-Trimethylbenzene (mesitylene)	1	9	120	1	165	50	0.00321	3.6
Trimethylbenzenes	1	9	120	1	170	59	0.00262	3.6
n-Propylbenzene	1	9	120	1	159	52	0.00444	3.7
Isopropylbenzene	1	9	120	1	154	50	0.00602	3.6
Ethyl-methylbenzenes (cumene)	1	9	120	1	163	85	0.00367	3.6
Isopropyl-4-methylbenzene	1	10	134	2	177	34	0.00201	4.1
Butylbenzenes	1	10	134	2	174	17.7	0.00225	4.1
Tetramethylbenzenes	1	10	134	2	200	3.48	0.00057	4.0

Both the solubility and toxicity of the nonaromatic hydrocarbons are much less than for the aromatics and dissolution (and water concentrations) of nonaromatics is safely ignored. Thus, dissolved concentrations are calculated only for each of the three soluble aromatic pseudocomponents. Tables 2 and 3 list physical–chemical characteristics of individual aromatics used to derive a mean molecular weight, boiling point, solubility, and vapor pressure for each of the three volatile and soluble or semisoluble aromatic pseudocomponents (Table 4). The vapor pressure used to characterize each of the volatile aliphatic pseudocomponents is equivalent to that for the aromatic pseudocomponent of the same boiling point range. This number of pseudocomponents provides sufficient accuracy for the evaporation and dissolution calculations, particularly given the time frame (minutes) over which dissolution occurs from small droplets and the rapid resurfacing of large droplets (see discussion above, this section).

The schematic in Figure 1 shows oil fate processes simulated in the model in open water. The oil (whole and as pseudocomponents) rapidly separates into different phases or parts of the environment, i.e., surface slicks; emulsified oil (mousse) and tar balls; oil droplets suspended in the water column; dissolved lower molecular weight components (MAHs and PAHs) in the water column; oil droplets adhered and hydrocarbons adsorbed to suspended particulate matter in the water; hydrocarbons on and in the sediments; dissolved MAHs and PAHs in the sediment pore water; and hydrocarbons on and in the shoreline sediments and surfaces.

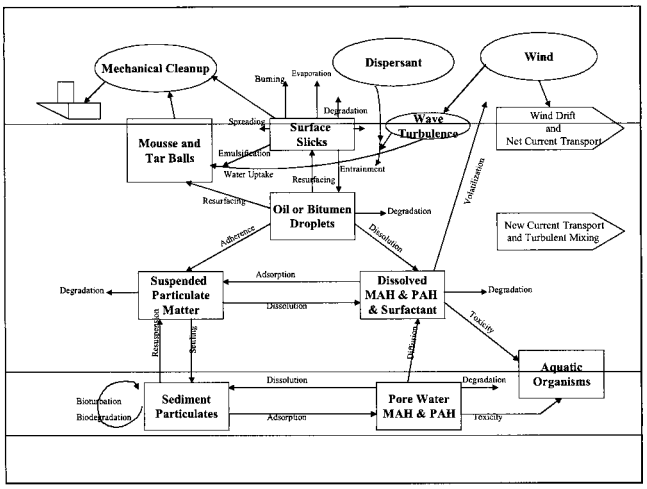

Fig. 1. Simulated oil fate processes in open water. Monoaromatic hydrocarbon (MAH); polycyclic aromatic hydrocarbon (PAH).

Transport

Separate Lagrangian elements (spillets) representing sublots of surface-floating oil, subsurface droplets, and dissolved components are used to simulate the movements of oil components in three dimensions over time. Transport is the sum of advective velocities of currents input to the model, surface wind drift (either using a constant percent of wind speed and deflection angle, typically observed as 3–4% and 0–10° to right of downwind in the Northern Hemisphere [1] or based on the model by Youssef and Spaulding [67]), and randomized turbulent diffusive velocities in two (floating oil) or three (subsurface oil) dimensions. The magnitudes of the directional components of randomized diffusion are scaled by horizontal and vertical diffusion coefficients [68] using a random walk technique [69]. The vertical diffusion coefficient (D_v, m²/s) in the wave-mixed layer is computed as a function of wind speed (at 10 m above the sea surface, W_{10}), based on Thorpe [70]:

$$D_v = 0.0015W_{10} \quad (1)$$

The horizontal and deeper water vertical diffusion coefficients are model inputs

Oil droplets also undergo vertical movements according to buoyancy using a modified Stoke's law. The rise velocity for each droplet size i, w_i (m/s), is

$$w_i = d_i^2 g(1 - \rho_o/\rho_w)/18\upsilon_w \quad (2)$$

where d_i is the droplet diameter (m), g is the gravitational acceleration (m/s²), ρ_o is the density of the oil (kg/m³), ρ_w is

Table 3. Physical–chemical properties for 2- to 4-ring polynuclear aromatic hydrocarbons. Molecular weight (MW), boiling point (BP), solubility, and vapor pressure are from Mackay et al. [64–66]. Estimates of log(K_{OW}) are based on Mackay et al. [63,64] and Neff and Burns [126]. (A dash indicates no data available)

Compound(s)	Rings	Cs	MW (g/mol)	Distillation cut no.	BP (°C)	Solubility (ppm)	Vapor pressure (atm)	Log(K_{OW})
Tetralin	2	10	132	2	208	15	0.00052	3.8
Diphenylmethane	2	13	168	2	264	16	8.73×10^{-07}	4.1
Biphenyl	2	12	154	2	261	5.53	1.28×10^{-05}	3.9
Naphthalene	2	10	128	2	218	31	0.00010	3.4
C1-naphthalenes	2	11	142	2	243	26.5	8.80×10^{-05}	3.9
C2-naphthalenes	2	12	156	2	254	6.4	1.98×10^{-05}	4.4
C3-naphthalenes	2	13	170	3	267	—	—	5.0
C4-naphthalenes	2	14	185	3	—	—	—	5.6
Acenaphthylene	3	12	152	3	270	16.1	8.88×10^{-06}	4.1
Acenaphthene	3	12	154	3	278	3.8	2.96×10^{-06}	3.9
Dibenzofuran	3	12 + O	168	3	287	4.75	2.96×10^{-06}	4.3
Fluorene	3	13	166	3	295	1.9	8.88×10^{-07}	4.2
C1-fluorenes	3	14	181	3	—	1.09	—	5.0
C2-fluorenes	3	15	196	3	—	—	—	5.2
C3-fluorenes	3	16	211	3	—	—	—	5.5
Anthracene	3	14	178	3	340	0.045	9.87×10^{-09}	4.5
Phenanthrene	3	14	178	3	339	1.1	1.97×10^{-07}	4.6
C1-phenanthrenes/anthracenes	3	15	192	3	—	—	—	5.1
C2-phenanthrenes/anthracenes	3	16	207	3	—	—	—	5.3
C3-phenanthrenes/anthracenes	3	17	222	4	—	—	—	6.0
C4-phenanthrenes/anthracenes	3	18	237	4	390	—	—	6.5
Dibenzothiophene	3	12 + S	184	3	333	—	—	4.5
C1-dibenzothiophene	3	13 + S	199	3	—	—	—	4.9
C2-dibenzothiophene	3	14 + S	214	3	—	—	—	5.5
C3-dibenzothiophene	3	15 + S	228	4	—	—	—	5.7
Fluoranthene	4	16	202	3	375	0.265	—	5.2
Pyrene	4	16	202	3	404	0.013	—	5.2
C1-fluoranthenes/pyrenes	4	17	217	4	407	—	—	5.7
Chrysene	4	18	228	4	448	0.0018	—	5.9
C1-Chrysenes	4	19	242	4			—	6.4

the density of the water (kg/m^3), and υ_w is the kinematic viscosity of water (m^2/s). This relation holds for low Reynolds numbers ($Re < 20$). The Reynolds number describes the degree of turbulence in the flow over the particle and is defined as $Re = Lv/\upsilon_w$, where L is the length scale (d_i in this case).

Shoreline stranding

The fate of spilled oil that reaches the shoreline depends on characteristics of the oil, the type of shoreline, and the energy environment. The stranding algorithm is based on data and analysis of Gundlach [71] and Reed and Gundlach [72]. In SIMAP, deposition occurs when an oil spillet intersects shore surface and ceases when the volume-holding capacity for the shore surface is reached. Because subsequent oil coming ashore is not allowed to remain on the shore surface, it is refloated and carried to sea by outgoing tidal currents and wind drift. The shoreline oil is then removed exponentially with time. Data for holding capacity and removal rate are taken from Gundlach [71] and are a function of oil viscosity and shore type. The algorithm and data are in French et al. [30]. Shore widths by shore type are data inputs to SIMAP.

Spreading

Spreading of floating oil is modeled in three ways. The rapid thinning and broadening of surface slicks caused by gravitational forces [73] is modeled as an increase in the diameter of each floating spillet according to the spreading algorithm empirically derived by Mackay et al. [17–19], who modified Fay's approach and described the oil as thin and thick slicks (as described in French et al. [30]). They assumed the thick slick feeds the thin slick and that 80 to 90% of the total slick area is represented by the thin slick. The formulation is corrected for number of surface spillets [24]. Spreading is stopped when an oil-specific terminal thickness is reached, based on data from McAuliffe [61], as described in Table 5.

In addition, oil spreads by so-called shear spreading, the entrainment and resurfacing of oil, whereby the oil is affected differentially by the wind drift and subsurface currents [74,75].

Table 4. Mean physical–chemical properties for each aromatic pseudo-component, based on data in Tables 2 and 3; see Table 3 for acronym definitions

Pseudo-component	Rings	Cs	MW (g/mol)	Distillation cut no.	BP (°C)	Solubility (ppm)	Vapor pressure (atm)	Log(K_{OW})
1-Ring aromatics	1	8.4	111	1	149	242.4	0.01525	3.3
2-Ring aromatics	1.7	10.9	142	2	222	17.3	6.20×10^{-04}	4.0
3-Ring aromatics	3.1	14.4	187	3	324	3.2	2.65×10^{-06}	4.8

Table 5. Minimum oil thickness for gravitational spreading based on data in McAuliffe [61]

Oil viscosity (mPa/s)	Minimum slick thickness (mm)
<10	0.01
10–20	0.05
20–1,000	0.1
>1,000	1

This later process was observed by Reed et al. [76] and in validation studies of SIMAP using test spills in the Caribbean Sea [27].

Finally, the use of multiple spillets to simulate releases over time and in more than one location (such as along a ship's path) effectively spreads the floating oil. Both surface and subsurface releases are modeled. For a subsurface release, the oil is initiated as droplets of an assigned droplet size distribution, the larger of which rise and surface over an area determined by the height of the water above the release point(s) and the currents in the water column.

Evaporation

The evaporation algorithm in SIMAP is based on accepted evaporation theory, which follows Raoult's law that each component evaporates at a rate proportional to the saturation vapor pressure and mole fraction present for that component. Each pseudocomponent evaporates according to its mean vapor pressure, solubility, and molecular weight (Table 4). The mass transfer coefficient is calculated using the methodology of Mackay and Matsugu [77], as described in French et al. [30] and analogous to that described by Jones [49]. Evaporation from surface and shoreline oil increases with the oil surface area, temperature, and wind speed. As lighter components evaporate off, the remaining weathered oil becomes more viscous.

Jones [49] compared the results of the pseudocomponent model to laboratory data in Fingas [78] and the model of Stiver and Mackay [79], who used an analytical approach to predict the volume fraction evaporated using distillation data to estimate needed parameters. The pseudocomponent model agreed with the Fingas data under nearly equivalent conditions (20 g of oil 1.5 mm thick and no wind). The pseudocomponent model predicts slightly lower evaporation rates than the Stiver and Mackay model, with the two models varying systematically (parallel as a function of temperature). The difference is accounted for by the approximation of vapor pressure from distillation data for the Stiver and Mackay model.

Emulsification

The formation of water-in-oil emulsions, or mousse, depends on sea state and the resin, asphaltene, and wax content of the oil [78,80–82]. Oils vary in their ability to form stable emulsions. Emulsified oil can contain as much as 80% water in the form of micrometer-sized droplets dispersed within a continuous phase of oil [78,83,84]. These authors argue that, for accuracy, an empirical approach with curves fit for each oil is needed to account for oil-specific emulsification rates and the degree of stability of the emulsion. However, for general applicability of SIMAP, emulsification (water-in-oil, i.e., mousse formation) is modeled using the scheme of Mackay and Zagorski [85], as described in French et al. [30]. Water content increases exponentially, with the rate related to the square of wind speed and previous water incorporation. Viscosity increases as water content increases in the oil, and the increasing viscosity feeds back in the model to slow the entrainment rate. As information becomes more available, a new water incorporation algorithm accounting for the oil's resin, asphaltene, and wax content, as well as the stability of the water-in-oil emulsion, should be developed.

Entrainment

Entrainment by surface-breaking waves is modeled based on Delvigne and Sweeney [86] who, using laboratory and flume experimental observations, developed a relationship for entrainment rate as a function of oil droplet size, which in turn is related to turbulent energy level (as breaking wave energy times fraction of the sea surface covered by breaking waves) and oil viscosity. The data and relationships in Delvigne and Sweeney [86] and Delvigne and Hulsen [87] are used to calculate mass and particle size distribution of droplets entrained:

$$Q_d = C^* D_d^{0.57} S F d^{0.7} \Delta d \quad (3)$$

where Q_d is the entrainment rate (kg/m^2-s) for droplet diameter d (m), C^* is an empirical entrainment constant that depends on oil type and weathering state, D_d is the dissipated breaking wave energy per unit surface area (J/m^2), S is the fraction of sea surface covered by oil, F is the fraction of sea surface hit by breaking waves, and Δd is the oil particle interval diameter (m). Using the data reported in Delvigne and Hulsen [87], the entrainment constant, C^*, was fit to the following:

$$\text{If } (\mu/\rho) < 132 \text{ cSt}, \qquad C^* = \exp[-0.1023 \ln(\mu/\rho_o) + 7.572] \quad (4)$$

$$\text{If } (\mu/\rho) \geq 132 \text{ cSt}, \qquad C^* = \exp[-1.8927 \ln(\mu/\rho_o) + 16.313] \quad (5)$$

where μ is the viscosity (mPa/s) and ρ_o is the density (g/cm^3) of the oil. The mean droplet diameter of entrained oil, d_{50} (μm), was fit with a curve to data in Delvigne and Sweeney [86] to yield:

$$d_{50} = 1{,}818 E^{-0.5} (\mu/\rho_o)^{0.34} \quad (6)$$

where E is the wave energy dissipation rate per unit volume (J/m^3-s) with E set at 10^3 (J/m^3-s) for breaking waves.

Delvigne and Sweeney [86] found that there is a linear relationship between $\log(N_i)$ and $\log(d_i)$, where N_i is the number of particles in the size interval $0.5d_i$ to d_i, and d_i is particle diameter. Thus, the relative distribution of numbers, and volume (or mass) for spherical droplets, can be calculated as a function of droplet size. It follows (Delvigne and Sweeney [86], Eqn. 4) that

$$\sum_{j=1}^{i-1} V_j = 1.45 V_i \quad (7)$$

where V_i is the volume in size class $0.5d_i$ to d_i, and V_j is the volume in each of the size classes smaller than $0.5d_i$ to d_i, and the sum is from j = 1 to (i − 1). This equation indicates a rapid decrease in volume as droplet size decreases. The minimum and maximum droplet diameters entrained in the water column are assumed to be $0.1d_{50}$ and d_{50}, respectively. The minimum is set at 10% d_{50} because volumes below this size are relatively small (about 2% of the volume in the mean size class), and can be neglected. The maximum value is set to equal the mean because, in numerical experiments and model

testing, droplets larger than d_{50} were found to resurface in less than one time step and so are not quantified as separate from surface slicks. In the model, six size classes are used, evenly distributed by diameter from the minimum to the maximum size. The dissipated wave energy, D_d (J/m^2), is

$$D_d = 0.0034\rho_w g H^2 \quad (8)$$

where ρ_w is the density of water (kg/m^3), g is the acceleration due gravity (m/s^2), and H is the root mean square value of breaking wave height (m). The fraction of the sea surface hit by breaking waves per unit time, F, is parameterized for $U_w \leq U_{th}$ [11] as

$$F = 3 \times 10^{-6}(U_w^{3.5}/T_w) \quad (9)$$

and, for $U_w > U_{th}$ [86] as

$$F = 0.032([U_w - U_{th}]/T_w) \quad (10)$$

where U_w is the wind speed at 10 m above the sea surface (m/s), U_{th} is the threshold wind speed for onset of breaking waves ($\sim$6 m/s), and T_w is the significant wave period (s). The total mass entrained into the water column in a time step Δt (sec), M_E (kg), is

$$M_E = A\Delta t \sum (Q_d \Delta d) \quad (11)$$

where A is the area of surface slick (m^2). The intrusion depth, Z_m (m), is

$$Z_m = (1.5 \pm 0.3)H_b \quad (12)$$

where H_b is the breaking wave height (m). Wave height is calculated from wind speed, duration, and fetch (distance upwind to land), using the algorithms from the Coastal Engineering Research Center [88]. The mixing depth (except where constrained by the seafloor) for each droplet size class, Z_i (m), is

$$Z_i = \max(D_v/w_i, Z_m) \quad (13)$$

where D_v is the vertical dispersion coefficient (Eqn. 1) and w_i is the rise velocity for the droplet size (Eqn. 2).

Entrainment rate is slower and droplet size is larger for higher viscosity oils and as oil viscosity increases by emulsification and evaporation loss of lighter volatile components. The droplet size determines how fast and whether the oil resurfaces. Droplets greater than 70 μm in diameter are assumed to float if they reach the water surface by vertical diffusion; smaller droplets reaching the surface are mixed downward if their rise velocity is overcome by the vertical diffusion velocity and resurface otherwise. The 70 μm threshold is based on observations by Lunel [89] of droplet sizes that seem to be dispersed permanently. Resurfaced oil typically forms sheens. As surface oil is blown downwind faster than the underlying water, resurfacing droplets come up behind the leading edge of the oil, effectively spreading the slicks in the downwind direction.

Waves break beginning at about 12 knots ($\sim$6 m/s) of wind speed and wave breaking increases as wind speed becomes higher. Thus, entrainment becomes increasingly important (higher rate of mass transfer to the water) the higher the wind speed. Below 12 knots of wind speed, the percentage of mass entrained is not significant. As wind and turbulence increase, the oil droplet sizes become smaller, although there is a feedback slowing of the entrainment process as oil weathers and/or emulsifies, becoming more viscous. Application of chemical dispersant decreases surface tension of the oil, and so increases the entrainment rate (at a give level of turbulence) and decreases droplet size. The droplet size distribution of chemically dispersed oil is based on observed sizes in Lunel [89]. Typically, dispersants are effective on oils up to a viscosity of about 10,000 mPa/s [13,14,83], a threshold above which entrainment is negated in the model.

Surf entrainment

Wave height in the surf zone may be input to the model to induce entrainment. The above algorithm based on Delvigne and Sweeney [86] is used to determine the droplet size distribution of surf-entrained oil, which is assumed well-mixed in the surf zone. Settling of particles does not occur in water depths where waves reach the bottom (taken as 1.5 multiplied by wave height).

Dissolution

The algorithm developed by Mackay and Leinonen [16] is used in SIMAP for dissolution from a surface slick. The slick (spillet) is treated as a flat plate, with a mass flux [90] related to solubility and temperature. It assumes a well-mixed layer with most of the resistance to mass transfer lying in a hypothetical stagnant region close to the oil. For subsurface oil, dissolution is treated as a mass flux across the surface area of a droplet (treated as a sphere) as in Mackay and Leinonen [16]. Dissolution rate increases the higher the surface area of the oil relative to its volume. Because the surface area–to–volume ratio is higher for smaller spherical droplets, dissolution is higher for smaller droplets. The droplet size distribution and amount of oil entrained, both functions of turbulence, are the critical determinants of dissolved concentrations. As discussed above, dissolution from entrained small droplets is much faster than from surface slicks in the shape of flat plates (which is insignificant). The soluble components also are volatile, and evaporation from surface slicks is faster than dissolution into the underlying water. Thus, the processes of evaporation and dissolution are competitive, with evaporation the dominant process for surface oil.

Volatilization

Volatilization of dissolved components from the water to the atmosphere occurs as they are mixed and diffuse to the sea surface boundary and enter the gas phase. Volatilization rate increases with increasing temperature. The procedure outlined by Lyman et al. [91], based on Henry's law and mass transfer [90], is followed in the model [30]. The volatilization depth for dissolved substances is limited to the maximum of one half the wave height.

Dissolved-suspended particulate partitioning, adherence, and sedimentation

Adsorption of dissolved components to particulate matter in the water occurs because the soluble components are only sparingly so. These compounds preferentially adsorb to particulates when the latter are present. The ratio of adsorbed to dissolved concentrations is computed from standard equilibrium partitioning theory [92]. Adsorption increases with $\log(K_{ow})$ and the concentration of suspended particulates, with the particulate phase accounting for a significant percentage of the mass above 100 mg/L suspended sediments.

The model formulation developed by Kirstein et al. [21] is used to calculate the volume of oil droplets adhered to particles. The Stoke's law formulation (Eqn. 2) is used to adjust

vertical position of oil–sediment particles, using the density of the combined particle. If turbulence subsides sufficiently, the oil–sediment agglomerates will settle.

Sedimentation occurs when oil–sediment agglomerates and particles with adsorbed semisoluble components (MAHs and PAHs) settle to the bottom sediments. Adherence and sedimentation can be an important pathway of oil in nearshore areas when waves are strong and subsequently subside. Generally, oil–sediment agglomerates transfer more PAH to the bottom than sediments with PAHs that were adsorbed from the dissolved phase in the water column. Resuspension of settled oil–sediment particles may occur if current speeds exceed threshold values where adhesive forces can be overcome, assumed 20 cm/s in the model.

Bioturbation

Bioturbation, the process where animals in the sediments mix the surface sediment layer while burrowing, feeding, or passing water over their gills, effectively mixes the surface sediment layer about 10 cm thick (in nonpolluted environments). In the model, sediment concentration is calculated as mass loading per area divided by 10 cm. Contaminant concentrations in sediment are distributed between adsorbed and dissolved states by equilibrium partitioning, as in the water column. For this calculation, the particulate-to-interstitial water ratio is taken to be 0.45 [88].

Degradation

Degradation includes biodegradation, photooxidation, and other chemical reactions. A first-order decay algorithm is used, with a specified (total) degradation rate for each of surface oil, water column oil, and sedimented oil. Degradation rates for the aromatics are from Mackay et al. [63–66] and for whole oil are from French et al. [30].

Fates model output

The physical fates model creates output files recording the distribution of a spilled substance in three-dimensional space and time as area covered by oil and thickness on the water surface (swept area); volumes in the water column at various concentrations of dissolved aromatics; volumes in the water column at various concentrations of total hydrocarbons in suspended droplets; total hydrocarbon concentrations and dissolved aromatic concentrations in surface sediment; and lengths and locations of shoreline impacted and volume of oil ashore in each segment. The dissolved aromatic hydrocarbon concentration in the water column is calculated from the mass in spillets representing dissolved components, as follows. Concentration is contoured on a three-dimensional Lagrangian grid system (of 200 $\times$ 200 cells in the horizontal and five vertical layers), which is scaled each time step to just cover the volume occupied by dissolved aromatic particles, including the dispersion around each spillet center. This maximizes the resolution of the concentrations at each time step and reduces error caused by averaging mass over large cell volumes. Distribution of mass around the spillet center is described as Gaussian in three dimensions, with one standard deviation equal to twice the diffusive distance ($2D_x t$ in the horizontal, $2D_z t$ in the vertical, where D_x is the horizontal and D_z is the vertical diffusion coefficient, and t is particle age). The plume grid edges are set at one standard deviation out from the outermost particle. These data are used by the biological effects model to evaluate exposure, toxicity, and impacts.

BIOLOGICAL EFFECTS MODEL

The biological exposure model estimates the area, volume, or portion of a stock or population affected by surface oil, concentrations of oil components in the water, or sediment contamination. The biological effects model estimates losses resulting from acute exposure after a spill (i.e., losses at the time of the spill and while acutely toxic concentrations remain in the environment) in terms of direct mortality and lost production because of direct exposure or the loss of food resources from the food web. Losses are estimated by species or species group for fish, invertebrates (i.e., shellfish and nonfished species), and wildlife (birds, mammals, sea turtles). Lost production of aquatic plants (microalgae and macrophytes) and lower trophic levels of animals also are estimated.

The area potentially affected by the spill is represented by a rectangular grid with each grid cell coded as to habitat type. The habitat grid also is used by the physical fates model to define the shoreline location and type, as well as habitat and sediment type. A habitat is an area of essentially uniform physical and biological characteristics that is occupied by a group of organisms that are distributed throughout that area. A contiguous grouping of habitat grid cells with the same habitat code represents an ecosystem in the biological model. Prespill abundance of fish, invertebrates, and wildlife, and rates of lower trophic level productivity, are assumed constant for the duration of the spill simulation and evenly distributed across an ecosystem. Though biological distributions are known to be highly variable in time and space, data generally are not sufficient to characterize this patchiness. Oil also is patchy in distribution. The patchiness is assumed to be on the same scale so that the intersection of the oil and biota is equivalent to overlays of spatial mean distributions.

Mobile fish, invertebrates, and wildlife are assumed to move at random within each ecosystem during the simulation period. This is a reasonable assumption for the period of the simulation (generally a few weeks). Benthic organisms also may remain stationary on or in the bottom. Planktonic stages, such as pelagic fish eggs, larvae, and juveniles (i.e., young-of-the-year during their pelagic stage[s]), move with the currents.

Habitats include open water, reef (coral or mollusk), wetland, sea grass, kelp bed, and shoreline environments. Habitat types are defined by depth, proximity to shoreline(s), bottom/shore type, dominant vegetation type, and the presence of invertebrate reefs. With respect to proximity to shoreline(s), habitats are designated as landward or seaward. Landward portions are the nearshore rivers, estuaries, and inlets. The seaward portion is the more oceanic or main part of the water body. This designation allows different biological abundances to be simulated in landward and seaward zones of the same habitat type (e.g., open water with sand bottom).

Wildlife

In the model, surface slicks (or other floating forms such as tar balls) of oils and petroleum products impact wildlife (birds, marine mammals, sea turtles, and other reptiles). For each of a series of surface spillets, the physical fates model calculates the location and size (radius of circular spreading spillet) as a function of time. The area swept by a surface spillet in a given time step is calculated as the quadrilateral area defined by the path swept by the spillet diameter. This area is summed over all time steps for the time period the spillet is present on the water surface and separately for each

Table 6. Combined probability of encounter with the slick and mortality once oiled, if present in the area swept by a slick exceeding a threshold thickness. Area swept is calculated for the habitats occupied

Wildlife group	Probability (%)	Habitats occupied
Dabbling waterfowl	99	Intertidal and landward subtidal
Nearshore aerial divers	35	Intertidal and landward subtidal
Surface seabirds	99	All intertidal and subtidal
Aerial seabirds	5	All intertidal and subtidal
Wetland wildlife (waders and shorebirds)	35	Wetlands, shorelines, seagrass beds
Cetaceans	0.1	Seaward subtidal
Furbearing marine mammals	75	All intertidal and subtidal
Pinnipeds, manatee, sea turtles	1	All intertidal and subtidal
Surface birds in seaward only	99	All seaward intertidal and subtidal
Surface diving birds in seaward only	35	All seaward intertidal and subtidal
Aerial divers in seaward only	5	All seaward intertidal and subtidal
Surface birds in landward only	99	All landward intertidal and subtidal
Surface diving birds in landward only	35	All landward intertidal and subtidal
Aerial divers in landward only	5	All landward intertidal and subtidal
Surface diving birds in water only	35	All subtidal
Aerial divers in water only	5	All subtidal

habitat type where the oil passes. Spillets sweeping the same area of water surface at the same time are superimposed. The total area swept over a threshold thickness by habitat type is multiplied by the probability that a species uses that habitat (0 or 1, depending upon its behavior) and a combined probability of oiling and mortality. This calculation is made for each surface-floating spillet and each habitat for the duration of the model simulation.

The portion of the wildlife in the area swept by the slick over a threshold thickness that are assumed to die is based on probability of encounter with the slick multiplied by the probability of mortality once oiled. The probability of encounter with the slick is related to the percentage of the time an animal spends on the water or shoreline surface. The probability of mortality once oiled is nearly 100% for birds and fur-covered mammals (assuming they are not treated successfully) and much lower for other wildlife. The products of the two probabilities for various wildlife behavior groups are in Table 6. Estimates for the probabilities were derived from information on behavior and field observations of mortality after spills [30]. The wildlife mortality model has been validated with more than 20 case histories, including the *Exxon Valdez* and other large spills, verifying that these values are reasonable [46,93]. (However, see discussion below in the *Validation* section.)

Area swept is calculated for the habitats occupied by each of the behavior groups of wildlife listed in Table 6. Species or species groups are assigned to behavior groups to evaluate their loss. The threshold is 10 microns ($\sim$10 g/m^2) thick oil, based on data on minimum dose to impact a bird and calculations described in French et al. [30]. Wildlife mortality is directly proportional to abundance per unit area and the percent mortalities in Table 6.

Fish, invertebrates, and aquatic plants

In the model, aquatic biota (fish, invertebrates, and plants in the water column and on/in the sediments) are affected by dissolved aromatic concentrations in the water or sediment. This rationale is supported by the fact that soluble aromatics are the most toxic constituents of oil [50–61,94]. Exposures in the water column are short in duration [51], therefore, effects there are the result of acute toxicity. In the sediments, exposure may be both acute and chronic, as the concentrations may remain elevated for longer periods of time. In either acute or chronic exposures, it is the aromatics, and specifically the PAHs, that cause effects either directly or indirectly via bioaccumulation and uptake via the food web [50].

The model evaluates mortality and sublethal effects of dissolved aromatic concentrations in the water or sediment. Mortality is a function of duration of exposure: The longer the duration of exposure, the lower the threshold for effects [30,60–62,95–101]. After a certain period of time, all individuals that will die at a given concentration have done so and no further mortality is observed. The lethal threshold concentration, also termed the incipient lethal level, is the concentration where mortality occurs after this sufficiently long exposure [95,102]. The incipient lethal concentration to 50% of exposed organisms, $LC50_\infty$, is the asymptotic LC50 reached after infinite exposure time (or long enough that that level is approached). The standard mortality model is utilized, with a lognormal relationship between percent mortality and concentration, and the LC50 the center of the distribution.

In SIMAP, $LC50_\infty$ is input to the model for the mixture of dissolved MAHs and PAHs originating from the type of oil spilled (see below). For each of a series of aquatic biota behavior groups, the model evaluates exposure duration, and corrects the LC50 for time of exposure and temperature to calculate mortality. Movements of biota, either active or by current transport, are accounted for in determining time and concentration of exposure. Lagrangian elements are used to represent schools or groups of animals. The elements move or remain stationary according to the behavior type, and concentration and duration of exposure are recorded. Exposures are integrated over space and time by habitat type to calculate a total percentage killed.

Behavior groups are used to represent species or stages within species covering the possible movement patterns (or lack thereof) for aquatic organisms, i.e., planktonic (moving with currents), demersal and stationary (on the bottom exposed to near bottom water), benthic (in the sediments and stationary), demersal fish and invertebrates (on the bottom exposed to near bottom water and moving slowly), small pelagic fish and invertebrates (moving randomly and slowly in the water column), and large pelagic fish and invertebrates (moving randomly and rapidly in the water column). Pelagic fish move at about 0.5 body length per second [103], which amounts to 9 km/d for a 20-cm small pelagic fish and 45 km/d for a 100-

cm large pelagic fish (sizes from French et al. [30]). For demersal species, movements are much slower, assumed to be 0.5 km/d. Demersal organisms always remain in the bottom layer within 1 m of the bottom, whereas pelagic fish move vertically within the water column. Lagrangian elements are used to distinguish organisms by behavior group and in six habitat types: Seaward (offshore) open water, landward (estuarine) open water, seaward (offshore) wetland and seagrass, landward (estuarine) wetland and seagrass, seaward (offshore) reef, and landward (estuarine) reef. These six habitat categories account for the fact that fish and other aquatic biota tend to prefer one or more of these types [30,104].

Mortality is calculated as percent loss by habitat and behavior group. This is translated into the equivalent area of 100% loss. That area may be divided by the total area of habitat available in the region of interest to estimate a percentage of a population affected. The percent mortality of the exposure group may be multiplied by abundance at the time exposed and in the habitat type to calculate the species' mortality as numbers or biomass (kg).

The mortality of each species is evaluated as a population loss using species-specific natural and fishing mortality rates and standard fisheries models. Production foregone is calculated as the lost growth the killed individuals would have undergone over their remaining life span. The population and production foregone models are described in French-McCay [46].

Lost production of plants and animals at the base of the food chain also is integrated in space and over time using the effective concentration to reduce growth to 50% of normal, to parameterize a lognormal function. For each time step and for each of the concentration grid cells output by the physical fates model, lost primary, zooplankton, and benthic production (P_L) are calculated as follows:

$$P_L = (1 - F_k)V/Z_d \times t \quad (14)$$

where F_k is the fraction of the uninhibited rate of production that is realized at the contaminant concentration, V is volume contaminated (m^3), Z_d is water depth, and t is the days contaminated. Total production loss is summed over time by habitat type and the integrated losses are summarized as m^2 − days of equivalent 100% loss of production. These may be multiplied by production rates (g dry wt m^{-2} d^{-1}) to estimate production losses. Lost production of dependent larger animals in the food web, due to reduction of food supply, is estimated using a simple food chain model [30]. Production losses of lower trophic levels typically are very small because of their short generation times and quick recovery after a spill. They have not been measured in the field because the impact is less than natural variability.

Oil toxicity

The following summarizes the oil toxicity model used to determine appropriate values of $LC50_\infty$ to input to the SIMAP exposure model. The full development of the oil toxicity model and data upon which it is based are in French-McCay [62]. The oil toxicity model utilizes the accepted toxic units approach for organic compounds whose primary acute effect is narcosis, which also is being used by the U.S. Environmental Protection Agency in the development of PAH water and sediment quality criteria [105,106]. The oil toxicity model has been validated using laboratory oil bioassay data [62].

It has been shown that toxicity of narcotic organic compounds, such as the lower-molecular-weight aromatics in oil (MAHs and PAHs), is related to K_{ow} [30,62,99,101,107–113]. Chemicals that have a narcotic mode of action impact organisms by accumulating in lipids (such as in the cell membranes) and disrupting cellular and tissue function, such that the more hydrophobic the compound the more accumulation and the more severe the impact. However, the more hydrophobic the compound, the less soluble it is in water, and so the less available it is to aquatic organisms. Compounds of $\log(K_{ow}) > 5.6$ are considered insoluble, and so are not bioavailable and thus not acutely toxic to aquatic biota [62]. Thus, impact is the result of a balance between bioavailability (dissolved-component exposure) and toxicity once exposed.

The acute toxic effects of narcotic chemicals are additive [30,62,105,106,113]. The Toxic Unit (*TU*) Model is used to estimate the toxicity of a mixture of narcotic chemicals, with *TU* defined as the exposure concentration divided by the LC50. For a mixture, the toxic units are additive: When $\Sigma TU = 1$, the mixture is lethal to 50% of exposed organisms.

It has been shown [62] that the LC50 of the mixture ($LC50_{mix}$) is related to the LC50 of each chemical i in the mixture and the fractional concentration of chemical i (F_i) in the total mixture:

$$F_i = C_{w,i} \Big/ \left(\sum C_{w,i} \right) \quad (15)$$

where $C_{w,i}$ is the dissolved concentration of chemical i in the water.

$$LC50_{mix} = 1 \Big/ \sum (F_i / LC50_i) \quad (16)$$

The values of F_i may be measured in the field or, if field samples are not available, F_i may be estimated from the source oil composition. French-McCay [62] showed that for surface waters, where turbulent entrainment of oil has occurred, the values of F_i nearly are proportional to the source oil aromatic composition. The $LC50_{mix}$ is calculated including those aromatics that are measured in the oil and dissolved in the water (with $\log(K_{ow}) \leq 5.6$) for long enough times for exposure to aquatic organisms to be significant. Typically (except for gasoline), only the PAHs are dissolved in sufficient quantity and remain in the water long enough for their *TU* values to be significant.

The values of $LC50_i$ for MAHs and PAHs were estimated using a regression model relating LC50 to K_{ow} [62], with the 95% confidence range of this regression providing LC50s for average (50th percentile), sensitive (2.5th percentile), and insensitive (97.5th percentile) species:

$$\log_{10}(LC50_\infty) = \log_{10}(\phi) + \gamma \log_{10}(K_{ow}) \quad (17)$$

Based on 278 bioassays on individual aromatics, the intercept and slope of the regression are: $\log_{10}(\phi) = 4.8926$ and $\gamma = -1.0878$. This regression describes the mean response for all species (i.e., the response of the average species). The slope of this relationship is constant for all species [106]. The intercept varies by species, with 95% of species falling within the range $\log_{10}(\phi) = 3.9704$ (sensitive species) and $\log_{10}(\phi) = 5.8147$ (insensitive species) [62].

The exponential decrease of LC50 with increasing duration of exposure is due to the accumulation of toxicant over time up to a critical body residue (tissue concentration) that causes mortality. The accumulation is more rapid at higher temperature, such that LC50 at a given (short) exposure time de-

creases with increasing temperature. The following algorithm was developed in French-McCay [62]:

$$LC50_{\infty} = LC50_t(1 - e^{-\varepsilon t}) \quad (18)$$

$$\log_{10}(\varepsilon) = \varepsilon_1 - \varepsilon_2 \log_{10}(K_{ow}) \quad (19)$$

$$d\varepsilon/dT = \tau T \quad (20)$$

where t is time of exposure, $LC50_t$ is LC50 at time t, $LC50_{\infty}$ is LC50 at infinite time of exposure, K_{ow} is the octanol–water partition coefficient, $\varepsilon_1 = 1.47$ and $\varepsilon_2 = 0.414$, T = temperature (C), and $\tau = 0.11$.

The SIMAP exposure model uses a rearrangement of Equation 18 to correct the LC50 for time of exposure and temperature, as recorded by movements of Lagrangian elements relative to toxic concentrations (i.e., greater than the concentration lethal to 1% of exposed organisms, LC1, approximated as 1% of $LC50_{\infty}$). Exposure time is the total time concentration exceeds LC1 and the concentration is the average over that time. The percent mortality is then calculated using the log-normal function centered on $LC50_t$.

The dissolved concentrations are estimated by the physical fates model for both the water column and sediments. Dissolved concentrations in the water column result mainly from dissolution of entrained oil droplets, as the soluble compounds evaporate faster from floating oil. In the sediments, exposure and mortality of benthic organisms are a function of the dissolved concentrations in pore water. This methodology has been validated by Swartz et al. [113] and used in sediment quality criteria for PAHs [106].

Impacts to habitats

Habitat impacts result from smothering by greater than a threshold thickness of oil on intertidal habitat or sediment areas or lethal concentrations of dissolved aromatics in the water column (e.g., for coral reef species forming the structural basis of the reef). The model performs these evaluations for each cell in the habitat grid. The threshold for smothering by whole oil is 14 mm, based on literature reviewed in French et al. [30]. The lethal dissolved concentration in the water column is the LC50 input to the model.

Long-term impacts from habitat loss are integrated in the biological effects model over the period of recovery. The recovery curve is simulated as a sigmoid function described by

$$\frac{dP_R}{dt} = a_r P_R(1 - P_R) \quad (21)$$

where P_R is portion recovered and a_r is a constant. The value of the constant a_r is derived from solution of the equation assuming P_R at $t = 0$ is 0.01 and P_R at $t = t_{rec}$ (the recovery time) is 0.99, whereupon Equation 21 may be solved as $P_R = 1/(1 + 99 \exp[-a_r t])$ with $a_r = 9.19/t_{rec}$. Recovery times by habitat are input to the model. Typical recovery periods are three years for benthic and intertidal habitats, 10 years for seagrass beds, 15 years for salt marshes, and 30 years for mangroves [30]. Impacts to dependant species and life stages are assumed proportional to lost habitat function (P_R), and production foregone is integrated over time to estimate a total impact.

VALIDATION

Summary of previous validation studies

The physical fates model has been validated with more than 30 case histories, including the *Exxon Valdez* and other large spills [46,93], as well as test spills designed to verify the model [27]. The validation studies show that the model is capable of hind-casting the oil trajectory and shoreline oiling, given accurate observed wind data following the spill and a reasonable depiction of surface currents, both tidal and background. As winds and currents are the primary forcing variables on oil fate, obtaining accurate data on these is very important to the accuracy of any simulation.

The biological effect model has been validated using simulations for 28 spill events where data are available for comparison [46,93]. In most cases [93] only the wildlife impacts could be verified because of limitations of the available observational data. However, in the *North Cape* spill simulations, both wildlife and water column impacts (lobsters) could be verified [46].

In most cases, impact information for the spill primarily consists of counts of rescued or dead wildlife. The model results either agree well with field estimates, or underestimate the observed kill. The cases where wildlife kills are underestimated are where an unusually high abundance of certain species occurred in the spill path, or where data on abundance of animals were not available. Many of these cases were in fact considered significant spills because of the presence of unusually high aggregations of certain wildlife species [93]. Modeling results show that the impact algorithms in the model are valid when input data on abundance are accurate. The uncertainty in the model results is proportional to uncertainty in abundance.

For the *North Cape* oil spill of January 1996 in Rhode Island, field observations were available for both surface and subsurface oil fates and impacts. The model's prediction of the oil's fate agreed with observations of surface oil movements and measurements of total hydrocarbons and aromatics in the water. The model estimate of birds oiled was 2,200 to 4,400, depending on the prespill abundance data assumed. (Uncertainty in the model results is proportional to that for the abundance estimates.) The midpoint of this range is 8.5 times the number of birds collected on beaches, in agreement with estimates for other spills. (The negotiated settlement used a factor of 6 for this spill.) Impacts on water column organisms were validated by comparison of the model estimate to the field observations of the lobster kill (8.3 million and 9 million, respectively) [46]. The model estimates of impacts to other marine species were used in the government's natural resource damage claim to the responsible party. This claim was settled based on these estimates of injury.

Exxon Valdez

The current version of the model, SIMAP, was used to simulate in more detail (than previously [93]) oil fates and biological effects from acute exposure to the *Exxon Valdez* oil spill (EVOS), as more information is available for this spill than any other in U.S. waters. Descriptions of the oil observations and ultimate fate are available from several sources [114–118]. The analysis and simulation was for oil fate processes and impacts occurring in Prince William Sound ([PWS] AK, USA) over the first 60 d after the release of 250,000 bbl (34.8×10^6 kg) of Alaskan North Slope crude oil on March 24, 1989, from 00:00 to 10:00 h (at Bligh Reef, 60.8°N, 146.88°W, Fig. 2).

Water temperature was 2°C and suspended sediment concentration was assumed 1 mg/L, a typical value for PWS [30]. Depth data for PWS were obtained from Hydrographic Survey

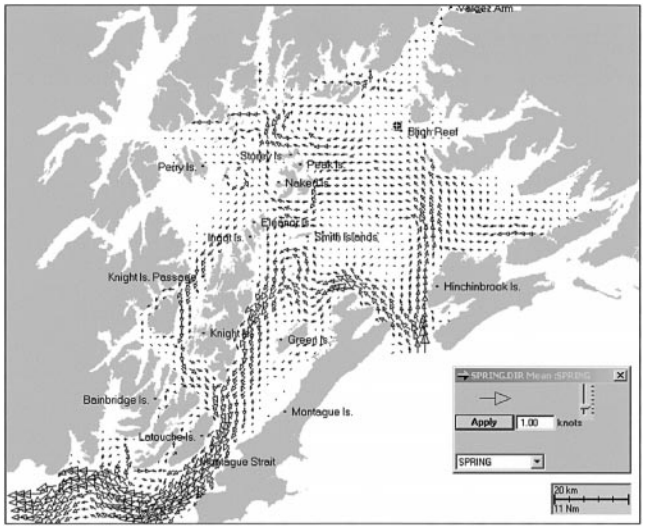

Fig. 2. Simulated currents in Prince William Sound (AK, USA) as a seasonal mean for spring. The spill site is indicated by the circled cross at Bligh Reef (AK, USA).

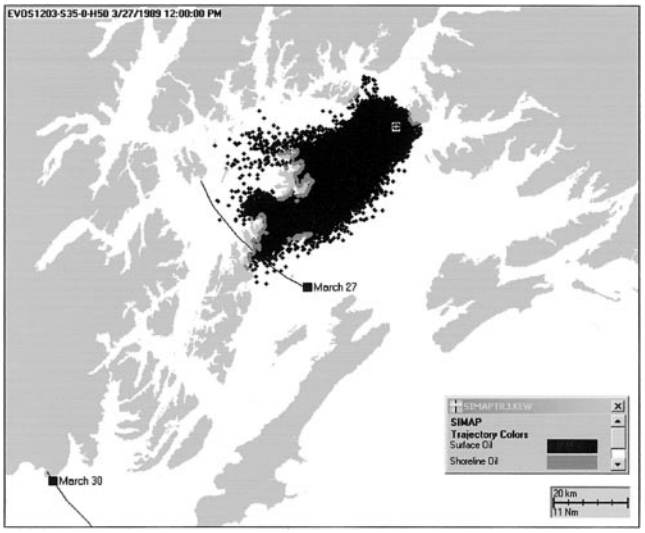

Fig. 3. Cumulative map of areas where surface-floating oil passed by March 27, 1989, at noon. The curved line on the map indicates the southwestward extent of observed oiling by this date.

Data supplied on CD-ROM by the U.S. Department of Commerce, National Oceanic and Atmospheric Administration (NOAA), National Geophysical Data Center. Shore types, available in digital form from the Environmental Sensitivity Atlas Geographical Information System (provided by NOAA, Hazardous Materials Response and Assessment Division, Seattle, WA, USA), were gridded with a cell size of 196 × 389 m, and the diagonal of 276 m assumed the length of a shore segment. Shore widths were assumed: 3 m for rocky, 10 m for gravel, 20 m for sand, and 300 m for wetlands [30].

A seasonal mean and tidal current field was simulated previously using a hydrodynamic model applied to PWS (Fig. 2 [23,119]). The boundary of the modeling domain was at the two entrances: Hinchinbrook Entrance and Montague Strait (AK, USA; Fig. 2). Tidal forcing functions for the major harmonic constituent (M2) and seasonal mean flows at the entrances were derived from the larger domain hydrodynamic model application for the Gulf of Alaska by Isaji and Spaulding [119]. This current field is similar to that used by Galt et al. [115] in their simulation of the spill. The flow generally was towards the southwest and out of PWS at Montague Strait (Fig. 2).

Wind data from several nearby stations in PWS were compiled [93], choosing the closest station to the floating oil on each date. On March 24 and 25, winds were light, but on March 26 there was a large windstorm involving strong northeasterly winds that emulsified and dispersed the oil widely in central PWS [115]. Wind drift was varied from 3 to 5% with angles applied from 0 to 20° to the right of downwind, with 3.5% and 0° proving to provide the best fit and timing of oil movements. The horizontal diffusion coefficient was varied from 10 to 100 m^2/s, which is a reasonable range for open waters and storm conditions [120]. The value 50 m^2/s provided the best fit to the observations. The vertical diffusion (randomized mixing) coefficient below the wave-mixed layer was assumed a typical 0.0001 m^2/s, but model results for this spill were insensitive to this parameter as water column contamination was very low.

Oil properties and pseudocomponent content were obtained from Environment Canada's Emergencies Science Division oil property database (Z. Wang, Environment Canada, Ottowa, ON, personal communication): Density, 0.8761 g/cm^3; viscosity, 16 mPa/s; surface tension, 27 dyne/cm; and maximum water content of mousse, 70%. The spilled oil was assumed to contain 30.66 g/kg MAHs; 3,750 mg/kg 2-ring PAHs; 6,622 mg/kg 3-ring PAHs; and 18.9%, 13.3% and 20.0% in aliphatic distillation cuts 1, 2, and 3, respectively. Thus, using these data, 4.1% of the oil potentially was toxic to aquatic biota and up to 56% of the oil could volatilize, dissolve, or biodegrade.

Figures 3 through 5 show cumulative maps for the simulation of areas where surface-floating oil passed during the first 60 d after the release. Figures 3 and 4 indicate the southwestward extent of oiling observed after the spill, as well as the model simulation. The model results are in agreement with observations: The oil remained near and just west of the spill site for the first 2 d (March 24 and 25). On March 26, during the windstorm, the oil emulsified and was dispersed and transported rapidly to the southwest, reaching the north end of Knight Island (AK, USA) by March 27. Floating oil was trans-

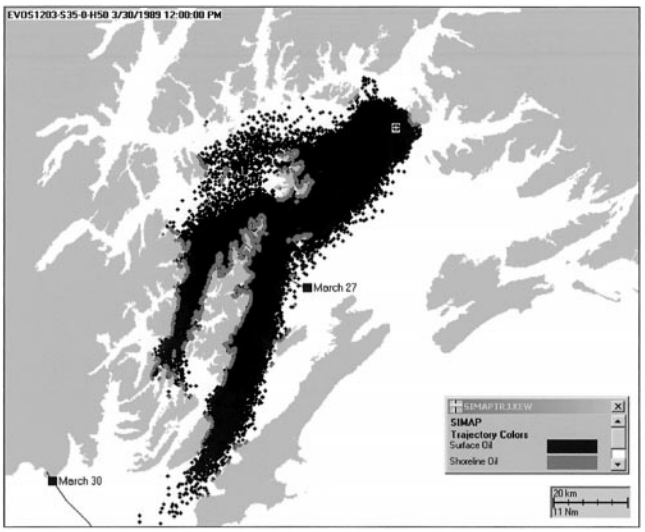

Fig. 4. Cumulative map of areas where surface-floating oil passed by March 30, 1989, at noon. The curved line on the map indicates the southwestward extent of observed oiling by this date.

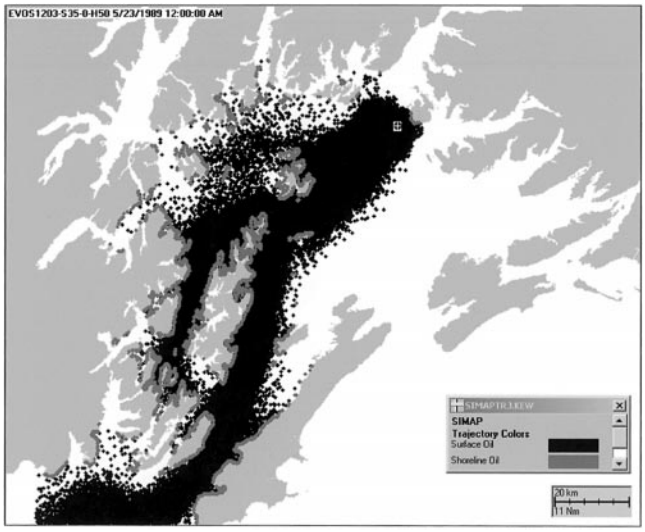

Fig. 5. Cumulative map of areas where surface-floating oil passed during the first 60 d after the release.

ported by prevailing southwesterly currents through Montague Strait, first exiting PWS on March 30. Oil continued to move generally in the southwesterly direction over the first two months, with wind-driven and localized dispersion causing shoreline oiling over a wide area (the modeled path in agreement with the summary map in Gundlach et al. [118]).

Table 7 summarizes the abundances of birds by species group occurring in seaward habitats affected in PWS [30]. The assumed probability of oiling was based on Table 6, the species feeding and sleeping behavior, and observations of avoidance of oil made by Day et al. [121]. Field estimates of the number of birds oiled in PWS (Table 7) were obtained using data in Piatt et al. [122] on the carcasses collected in PWS, divided by the probability of a killed bird being found in PWS, 35% (accounting for loss at sea, scavenging, search effort, and success), from Ford et al. [123]. Schempf et al. [124] estimated 192 bald eagles oiled in PWS, a factor 6 times the number of carcasses collected.

Model-estimated bird kills were in good agreement for species groups that were not observed to avoid oil. For those where avoidance was observed, model estimates were a factor 4 to 5 higher than the field estimates. Likely the probability of oiling is lower than the assumed 35% for these species, and 7 to 9% probability would fit the observations. However, the uncertainty of the abundance data is on the order of a factor of 2 or more as well. Thus, it could be error in abundance estimates and/or probability of oiling that accounts for the differences.

The model estimates were 3,555 otters and 26 seals oiled with PWS. The government estimates for all areas were 3,500 to 5,500 sea otters and 200 seals [125]. Most of the otters were impacted in PWS, but seals were impacted in other areas as well as inside PWS. Thus, the model estimates of impacts for these marine mammals are reasonable.

CONCLUSION

Success of a model simulation is dependent on both the algorithms and the accuracy of the input data. The validation exercises verified that the model algorithms provide reasonable results. The most important input data in determining accuracy of the physical fates model results are winds, currents, and assumed randomized diffusion rates. These data can be accurately estimated with appropriate measurements and hydrodynamic modeling.

With respect to the biological effects model, the results are sensitive to the assumed toxicity (LC50s), probability of oiling (including avoidance behavior), and biological abundances of the affected species. The range of toxicity values is well understood, based on the analysis in French-McCay [62]. However, few species have been measured in bioassays such that their degree of sensitivity to oil hydrocarbons is known. Performance of bioassays on individual aromatics, which logistically are easier to perform than with whole oil, would provide the necessary data to determine species sensitivity.

Estimation of biological abundance always will be uncertain due to the natural patchiness and variability of species distributions. In many analyses, such as in ecological risk assessments, evaluation of percent losses for populations of interest may be the appropriate measure of impact. This would avoid the difficulty of quantifying abundance at the time and location of the spill.

The probabilities of oiling, given oil passing through an area where wildlife are present, are based on limited data available in the literature. More detailed and quantitative information on bird and other wildlife behavior in the presence of

Table 7. Abundances of bird species groups in seaward habitats affected by the Exxon Valdez oil spill in Prince William Sound (AK, USA) [30], assumed probability of oiling, avoidance behavior (based on Day et al. [121]), estimated number killed based on field data (based on Piatt et al. [122], Schempf et al. [124], and Ford et al. [123]), and model estimated kill

Species group	No./km^2	Probability (%)	Avoid oil	No. killed (field)	No. killed (model)	Model/field
Loons	0.138	99	No	835	389	0.5
Grebes	0.337	35	(Some spp.)	1,132	563	0.5
Sea ducks	6.005	35	Yes	2,389	9,313	3.9
Procellariids	0.021	35	No	384	22	0.1
Cormorants	0.631	35	Yes	1,535	946	0.6
Gulls	4.013	5	Yes	173	687	4.0
Murres	4.672	35	Yes	1,458	5,282	3.6
Murrelets	2.767	35	Yes	1,113	5,369	4.8
Guillemots	0.182	99	No	451	514	1.1
Puffins	0.003	99	No	—	9	—
Other alcids	0.048	99	No	77	137	1.8
Eagles	2.323	35	Yes	192	34	0.2
Total birds	21.141	—	—	9,940	23,264	2.3

oil would improve greatly the knowledge base and ability to estimate impacts from spills. As the largest impacts of oil spills typically are to birds and fur-bearing marine mammals, these data needs are all the more pertinent.

The biological effects model in SIMAP evaluates exposure, considering movements and amounts of both oil and biota; impacts of response activities, such as booming and dispersant use; acute effects (lethal and sublethal) in the short-term; indirect effects of acute exposure via reduction in food supply or habitat; and nondensity-dependent population level impacts caused by mortality and sublethal effects. What have yet to be addressed in a quantitative manner are sublethal effects of chronic contamination; indirect effects via changes in ecosystem structure; and behavioral changes resulting in reduced growth, survival, or reproductive success. The latter are dependent on understanding of population and/or ecosystem structure and dynamics, areas of active study that are difficult to quantify but a challenge for future research.

Acknowledgement—The SIMAP Model has been developed over many years with the assistance and advice of many individuals at Applied Science Associates. The contributions of M. Reed, E. Anderson, D. Mendelsohn, M. Spaulding, V. Kolluru, T. Isaji, E. Howlett, H. Rines, C. Galagan, N. Whittier, J. Rowe, and T. Giguere are recognized and appreciated.

REFERENCES

1. Huang JC, Monastery FC. 1982. Review of the state of the art of oil spill simulation models. Final Report. American Petroleum Institute, Washington, DC.
2. Huang JC. 1983. A review of the state of the art of oil spill fate/behavior models. *Proceedings*, 1983 International Oil Spill Conference, San Antonio, TX, USA, February 28–March 3, American Petroleum Institute, Washington, DC, pp 313–322.
3. Spaulding ML. 1988. A state-of-the-art review of oil spill trajectory and fate modeling. *Oil Chem Pollut* 4:39–55.
4. American Society of Civil Engineers Task Committee on Modeling of Oil Spills. 1996. State-of-the-art review of modeling transport and fate of oil spills. *J Hydraulic Eng-ASCE* 122:594–609.
5. Reed M, Johansen O, Brandi PJ, Doling P, Lewis A, Fiasco R, Mackay D, Prentiss R. 1999. Oil spill modeling towards the close of the 20th century: Overview of the state-of-the-art. *Spill Science and Technology Bulletin* 5:3–16.
6. Yapa PD, Shen HT, Wang DS, Angammana K. 1992. An integrated computer model for simulating oil spills in the St. Lawrence River. *J GT Lakes Res*:34–51.
7. LaBelle RP, Johnson WR. 1993. Stochastic oil spill analysis for Cook Inlet/Shelikof Strait. *Proceedings*, 16th Arctic Marine Oil Spill Program Technical Seminar, Calgary, AB, June 7–9. Emergencies Science Division, Environment Canada, Ottawa, ON, pp 573–585.
8. Leech M, Walker M, Wiltshire M, Tyler A. 1993. OSIS: A Windows 3 oil spill information system. *Proceedings*, 16th Arctic Marine Oil Spill Program Technical Seminar, Calgary, AB, Canada, June 7–9. Emergencies Science Division, Environment Canada, Ottawa, ON, pp 549–572.
9. Proctor R, Elliott AJ, Flather R. 1994. Forecast and hindcast simulations of the *Braer* oil spill. *Mar Pollut Bull* 28:219–229.
10. Lehr WJ. 1996. Progress in oil spread modeling. *Proceedings*, 19th Arctic and Marine Oil Spill Program Technical Seminar, Calgary, AB, Canada, June 12–14. Emergencies Science Division, Environment Canada, Ottawa, ON, pp 889–894.
11. Lehr WJ, Overstreet R, Jones R, Watabayashi G. 1992. ADIOS—Automatic data inquire for oil spill. *Proceedings*, 15th Arctic and Marine Oil Spill Program Technical Seminar, Edmonton, AB, Canada, June 9–11. Emergencies Science Division, Environment Canada, Ottawa, ON, pp 31–45.
12. Lehr WJ, Wesley D, Simecek-Beatty D, Jones R, Kachook G, Lankford J. 2000. Algorithm and interface modifications of the NOAA oil spill behavior model. *Proceedings*, 23rd Arctic and Marine Oil Spill Program Technical Seminar, Vancouver, BC, Canada, June 14–16. Emergencies Science Division, Environment Canada, Ottawa, ON, pp 525–539.
13. Aamo OM, Reed M, Daling P. 1993. A laboratory-based weathering model: PC version for coupling to transport models. *Proceedings*, 16th Arctic Marine Oil Spill Program Technical Seminar, Calgary, AB, Canada, June 7–9. Emergencies Science Division, Environment Canada, Ottawa, ON, pp 617–626.
14. Daling PS, Aamo OM, Lewis A, Strom-Kritiansen T. 1997. SINTEF/IKU oil-weathering model: Predicting oil's properties at sea. *Proceedings*, 1997 International Oil Spill Conference, Fort Lauderdale, FL, USA, April 6–9. API Publication 4651. American Petroleum Institute, Washington, DC, pp 297–307.
15. Kolpack RL, Plutchak NB, Stearns RW. 1977. Fate of oil in a water environment—Phase II, a dynamic model of the mass balance for released oil. API Publication 4313. University of Southern California, American Petroleum Institute, Washington, DC.
16. Mackay D, Leinonen PJ. 1977. Mathematical model of the behavior of oil spills on water with natural and chemical dispersion. Economic and Technical Review Report EPS-3-EC-77-19. Fisheries and Environment Canada, Ottawa, ON.
17. Mackay D, Buist I, Mascarenhas R, Paterson S. 1980. Oil spill processes and models. Report EE-8. Environmental Emergency Branch, Department of Fisheries and Environment, Environment Canada, Ottawa, ON.
18. Mackay D, Paterson S, Trudel K. 1980. A mathematical model of oil spill behavior. Environmental Emergency Branch, Department of Fisheries and Environment, Environment Canada, Ottawa, ON.
19. Mackay D, Shiu WY, Hossain K, Stiver W, McCurdy D, Peterson S. 1982. Development and calibration of an oil spill behavior model. Report CG-D-27-83. U.S. Coast Guard, Research and Development Center, Groton, CT.
20. Mackay D, McAuliffe CD. 1988. Fate of hydrocarbons discharged at sea. *Oil Chem Pollut* 5:1–20.
21. Kirstein BE, Clayton JR, Clary C, Payne JR, McNabb D Jr, Fauna G, Redding R. 1987. Integration of suspended particulate matter and oil transportation study. OCS Study MMS87-0083. Minerals Management Service, Anchorage, AK, USA.
22. Daling PS, Mackay D, Mackay N, Brandvik PJ. 1990. Droplet size distributions in chemical dispersion of oil spills: Towards a mathematical model. *Oil Chem Pollut* 7:173–198.
23. Anderson E, Howlett E, Knauss W, French DP, Spaulding ML, Reed M, Puckett S, Isaji T, Mendelsohn D. 1990. The Alyeska tactical oil spill model. *Mar Technol Soc J* 24:33–39.
24. Kolluru V, Spaulding ML, Anderson E. 1994. A three-dimensional subsurface oil dispersion model using a particle-based approach. *Proceedings*, 17th Arctic and Marine Oil Spill Program Technical Seminar, Vancouver, BC, Canada, June 8–10. Emergencies Science Division, Environment Canada, Ottawa, ON, pp 815–835.
25. Spaulding ML, Howlett E, Anderson EL, Jayko K. 1992. OILMAP: A global approach to spill modeling. *Proceedings*, 15th Arctic Marine Oil Spill Program Technical Seminar, Edmonton, AB, Canada, June 9–11. Emergencies Science Division, Environment Canada, Ottawa, ON, pp 15–21.
26. Spaulding ML, Kolluru V, Anderson E, Howlett E. 1994. Application of three-dimensional oil spill model (WOSM/OILMAP) to hindcast the *Braer* spill. *Spill Science and Technology Bulletin* 1:23–35.
27. French DP, Rines H, Masciangioli P. 1997. Validation of an Orimulsion spill fates model using observations from field test spills. *Proceedings*, 20th Arctic and Marine Oil Spill Program Technical Seminar, Vancouver, BC, Canada, June 10–13. Emergencies Science Division, Environment Canada, Ottawa, ON, pp 933–961.
28. Reed M, Daling PS, Brakstd OG, Singsaas I, Faksness LG, Hetland B, Efrol N. 2000. OSCAR 2000: A multicomponent 3-dimensional oil spill contingency and response model. *Proceedings*, 23rd Arctic Marine Oil Spill Program Technical Seminar, Vancouver, BC, Canada, June 14–16, 1992. Emergencies Science Division, Environment Canada, Ottawa, ON, pp 663–952.
29. U.S. Department of the Interior. 1996. CERCLA Natural Resource Damage Assessment, Type A, Final Rule. *US Fed Reg* 61:20559–20614.
30. French D, Reed M, Jayko K, Feng S, Rines H, Pavignano S,

Isaji T, Puckett S, Keller A, French FW III, Gifford D, McCue J, Brown G, MacDonald E, Quirk J, Natzke S, Bishop R, Welsh M, Phillips M, Ingram BS. 1996. The CERCLA type A natural resource damage assessment model for coastal and marine environments (NRDAM/CME), technical documentation, Vols 1–6. Contract 14-0001-91-C-11. Final Report. U.S. Department of the Interior, Office of Environmental Policy and Compliance, Washington, DC.

31. Reed M, Spaulding ML. 1984. Response of Georges Bank cod to periodic and nonperiodic oil spill events. *Environ Manag* 8: 67–74.
32. Reed M, French DP, Calambokidis J, Cubbage J. 1989. Simulation modelling of the effects of oil spills on population dynamics of northern fur seals. *Ecol Model* 49:49–71.
33. Spaulding ML, Saila SB, Lorda E, Walker HA, Anderson EL, Swanson JC. 1983. Oil spill fishery interaction modelling: Application to selected Georges Bank fish species. *Estuar Coast Shelf Sci* 16:511–541.
34. Spaulding ML, Reed M, Anderson E, Isaji T, Swanson JC, Saila S, Lorda E, Walker H. 1985. Oil spill fishery impact assessment model: Sensitivity to spill location and timing. *Estuar Coast Shelf Sci* 20:41–53.
35. Laevastu T, Fukuhara F, eds. 1984. Quantitative determination of the effects of oil development in the Bristol Bay region on the commercial fisheries in the Bering Sea. NWAFC Processed Report 84-06. U.S. Department of Commerce, National Marine Fisheries Service, Northwest and Alaska Fisheries Center, Seattle, WA.
36. Trudel BK. 1984. A mathematical model for predicting the ecological impact of treated and untreated oil spills. In Allen TE, ed, *Oil Spill Chemical Dispersants.* STP 340. American Society for Testing and Materials, Philadelphia, PA, USA, pp. 390–413.
37. Trudel BK, Belore RC, Jessiman BJ, Ross SL. 1989. A microcomputer-based spill impact assessment system for untreated and chemically dispersed oil spills in the U.S. Gulf of Mexico. *Proceedings,* Oil Spill Conference, San Antonio, TX, USA, February 13–16, American Petroleum Institute, Washington, DC, pp 139–151.
38. Jayko K, Reed M, Bowles A. 1990. Simulation of interactions between migrating whales and potential oil spills. *Environ Pollut* 63:97–127.
39. Samuels WB, Lanfear KJ. 1982. Simulations of seabird damage and recovery from oil spills in the northern Gulf of Alaska. *J Environ Manag* 15:169–182.
40. Ford RG. 1985. A risk analysis model for marine mammals and seabirds: A southern California Bight scenario. MMS 85-0104. Final Report. U.S. Department of the Interior, Minerals Management Service, Pacific OCS Region, Los Angeles, CA.
41. Ford RG. 1987. Estimating mortality of seabirds from oil spills. *Proceedings,* 1987 Oil Spill Conference, Baltimore, MD, USA, April 6–9. American Petroleum Institute, Washington, DC, pp 547–551.
42. Ford RG, Wiens JA, Heinemann D, Hunt GL. 1982. Modelling the sensitivity of colonially breeding marine birds to oil spills: Guillemot and kittiwake populations on the Pribilof Islands, Bering Sea. *J Appl Ecol* 19:1–31.
43. Brody A. 1988. A simulation model for assessing the risks of oil spills to the California sea otter population and an analysis of the historical growth of the population. In Siniff DB, Ralls K, eds, *Population Status of California Sea Otters.* Contract 14-12-001-30033. U.S. Department of the Interior, Minerals Management Service, Pacific Outer Continental Shelf Region, Los Angeles, CA, pp 191–274.
44. French DP, Reed M, Calambokidis J, Cubbage J. 1989. A simulation model of seasonal migration and daily movements of the northern fur seal, *Callorhinus ursinus*. *Ecol Model* 48:193–219.
45. Seip KL, Sandersen E, Mehlum F, Ryssdel J. 1991. Damages to seabirds from oil spills: Comparing simulation results and vulnerability indexes. *Ecol Model* 53:39–59.
46. French-McCay DP. 2003. Development and application of damage assessment modeling: Example assessment for the *North Cape* oil spill. *Mar Pollut Bull* 47:341–359.
47. Payne JR, Kirstein BE, McNabb GD Jr, Lambach JL, Redding R, Jordan RE, Hom W, deOliveria C, Smith GS, Baxter DM, Gaegel R. 1984. Multivariate analysis of petroleum weathering in the marine environment—Sub-Arctic, Environmental Assessment of the Alaskan Continental Shelf, OCEAP. Final Report of Principal Investigators, Vols 21 and 22. U.S. Department of Commerce, National Oceanic, and Atmospheric Administration, Ocean Assessment Division, Juneau, AK.
48. Payne JR, Kirstein BE, Clayton JR Jr, Clary C, Redding R, McNabb GD Jr, Farmer G. 1987. Integration of suspended particulate matter and oil transportation study. Contract 14-12-0001-30146. Final Report. U.S. Department of the Interior, Minerals Management Service, Alaska OCS Region, Anchorage, AK.
49. Jones RK. 1997. A simplified pseudo-component oil evaporation model. *Proceedings,* 20th Arctic and Marine Oil Spill Program Technical Seminar, Vancouver, BC, Canada, June 10–13. Emergencies Science Division, Environment Canada, Ottawa, ON, pp 43–61.
50. National Research Council. 1985. *Oil in the Sea: Inputs, Fates, and Effects.* National Academy, Washington, DC, USA.
51. National Research Council. 2002. *Oil in the Sea III: Inputs, Fates and Effects.* National Academy, Washington, DC, USA.
52. Neff JM, Anderson JW, Cox BA, Laughlin RB Jr, Rossi SS, Tatem HE. 1976. Effects of petroleum on survival respiration and growth of marine animals. In *Sources, Effects, and Sinks of Hydrocarbons in the Aquatic Environment.* American Institute of Biological Sciences, Washington, DC, pp 515–539.
53. Neff JM, Anderson JW. 1981. *Response of Marine Animals to Petroleum and Specific Petroleum Hydrocarbons.* Applied Science, London and Halsted Press Division, John Wiley, New York, NY, USA.
54. Capuzzo JM. 1987. Biological effects of petroleum hydrocarbons: Assessments from experimental results. In Boesch DF, Rabulais NN, eds, *Long-Term Environmental Effects of Offshore Oil and Gas Development.* Elsevier, New York, NY, USA, pp 343–410.
55. Rice SD, Short JW, Karinen JF. 1977. Comparative oil toxicity and comparative animal sensitivity. In Wolfe DA, ed, *Fate and Effects of Petroleum Hydrocarbons in Marine Ecosystems and Organisms.* Pergamon, New York, NY, USA, pp 78–94.
56. Rice SD, Moles A, Taylor TL, Karinen JR. 1979. Sensitivity of 39 Alaskan marine species to Cook Inlet crude and No. 2 fuel oil. *Proceedings,* 1979 Oil Spill Conference, Los Angeles, CA, USA, March 19–22. American Petroleum Institute, Washington, DC, pp 549–554.
57. Tatem HE, Cox BA, Anderson JW. 1978. The toxicity of oils and petroleum hydrocarbons to estuarine crustaceans. *Estuar Coast Mar Sci* 6:365–373.
58. Malins DC, Hodgins HO. 1981. Petroleum and marine fishes: A review of uptake, disposition, and effects. *Envir Sci Technol* 15:1272–1280.
59. Anderson JW. 1985. Toxicity of dispersed and undispersed Prudhoe Bay crude oil fractions to shrimp, fish, and their larvae. Publication 4441. American Petroleum Institute, Washington, DC.
60. Anderson JW, Riley RG, Kiesser SL, Gurtisen J. 1987. Toxicity of dispersed and undispersed Prudhoe Bay crude oil fractions to shrimp and fish. *Proceedings,* 1987 Oil Spill Conference, Baltimore, MD, USA, April 6–9. American Petroleum Institute, Washington, DC, pp 235–240.
61. McAuliffe CD. 1987. Organism exposure to volatile/soluble hydrocarbons from crude oil spills—A field and laboratory comparison. *Proceedings,* 1987 Oil Spill Conference, Baltimore, MD, USA, April 6–9. American Petroleum Institute, Washington, DC, pp 275–288.
62. French-McCay DP. 2002. Development and application of an oil toxicity and exposure model, OilToxEx. *Environ Toxicol Chem* 21:2080–2094.
63. Mackay D, Shiu WY, Ma KC. 1992. *Illustrated Handbook of Physical–chemical Properties and Environmental Fate for Organic Chemicals,* Vol 1—Monoaromatic Hydrocarbons, Chlorobenzenes, and PCBs. Lewis, Boca Raton, FL, USA.
64. Mackay D, Shiu WY, Ma KC. 1992b. *Illustrated Handbook of Physical–chemical Properties and Environmental Fate for Organic Chemicals,* Vol 2—Polynuclear Aromatic Hydrocarbons, Polychlorinated Dioxins, and Dibenzofurans. Lewis, Boca Raton, FL, USA.
65. Mackay D, Shiu WY, Ma KC. 1992c. *Illustrated Handbook of Physical–chemical Properties and Environmental Fate for Organic Chemicals,* Vol 3—Volatile Organic Chemicals. Lewis, Boca Raton, FL, USA.

66. Mackay D, Shiu WY, Ma KC. 1992d. *Illustrated Handbook of Physical–chemical Properties and Environmental Fate for Organic Chemicals.* Vol 4—Oxygen-, Nitrogen-, and Sulfur-Containing Compounds. Lewis, Boca Raton, FL, USA.
67. Youssef M, Spaulding ML. 1993. Drift current under the action of wind waves. *Proceedings,* 16th Arctic Marine Oil Spill Program Technical Seminar, Calgary, AB, Canada, June 7–9. Emergencies Science Division, Environment Canada, Ottawa, ON, pp 587–615.
68. Okubo, A. 1971. Oceanic diffusion diagrams. *Deep-Sea Res* 8: 789–802.
69. Bear J, Verruijt A. 1987. *Modeling Groundwater Flow and Pollution with Computer Programs for Sample Cases.* Kluwer Academic, London, UK.
70. Thorpe SA. 1984. On the determination of K_v in the near surface ocean from acoustic measurements of bubbles. *J Phys Oceanogr* 14:861–863.
71. Gundlach ER. 1987. Oil holding capacities and removal coefficients for different shoreline types to computer-simulated spills in coastal waters. *Proceedings,* 1987 Oil Spill Conference, Baltimore, MD, USA, April 6–9. American Petroleum Institute, Washington, DC, pp 451–457.
72. Reed M, Gundlach E. 1989. Hindcast of the Amoco Cadiz event with a coastal zone oil spill model. *Oil Chem Pollut* 5:451–476.
73. Fay JA. 1971. Physical processes in the spread of oil on a water surface. In *Proceedings,* Joint Conference and Control of Oil Spills, June 15–17, Washington, DC.
74. Johansen O. 1984. The Halten Bank experiment—Observations and model studies of drift and fate of oil in the marine environment. *Proceedings,* 11th Arctic Marine Oil Spill Program Technical Seminar, Vancouver, BC, Canada, June 7–9, 1992. Emergencies Science Division, Environment Canada, Ottawa, ON, pp 18–36.
75. Elliot AJ, Hurford N, Penn CJ. 1986. Shear diffusion and the spreading of oil slicks. *Mar Pollut Bull* 17:308–313.
76. Reed M, Turner C, Odulo A. 1994. The role of wind and emulsification in modeling oil spill and drifter trajectories. *Spill Sci Technol Bull* 1:143–157.
77. Mackay D, Matsugu RS. 1973. Evaporation rates of liquid hydrocarbon spills on land and water. *Can J Chem Eng* 51:434–439.
78. Fingas M. 1995. Water-in-oil emulsion formation: A review of physics and mathematical modelling. *Spill Science and Technology Bulletin* 2:55–59.
79. Stiver W, Mackay D. 1984. Evaporation rate of oil spills of hydrocarbons and petroleum mixtures. *Environ Sci Technol* 18: 834–840.
80. Payne JR, McNabb GD Jr. 1984. Weathering of petroleum in the marine environment. *Marine Technology Society Journal* 18:24–42.
81. Payne JR, Phillips CR. 1985. *Petroleum Spills.* Lewis, Boca Raton, FL, USA.
82. Payne JR, Phillips CR. 1985. Photochemistry of petroleum in water. *Environ Sci Technol* 19:569–579.
83. Daling PS, Brandvik PJ. 1988. A study of the formation and stability of water-in-oil emulsions. *Proceedings,* 11th Arctic Marine Oil Spill Program Technical Seminar, Vancouver, BC, Canada, June 7–9, 1992. Emergencies Science Division, Environment Canada, Ottawa, ON, pp 153–170.
84. Fingas M, Fieldhouse B, Mullin JV. 1997. Studies of water-in-oil emulsions: Stability studies. *Proceedings,* 20th Arctic and Marine Oil Spill Program Technical Seminar, Vancouver, BC, Canada, June 10–13. Emergencies Science Division, Environment Canada, Ottawa, ON, pp 21–42.
85. Mackay D, Zagorski W. 1982. Water-in-oil emulsions. Environment Canada Manuscript Report EE-34. Environment Canada, Ottawa, ON.
86. Delvigne GAL, Sweeney CE. 1988. Natural dispersion of oil. *Oil Chem Pollut* 4:281–310.
87. Delvigne GAL, Hulsen LJM. 1994. Simplified laboratory measurements of oil dispersion coefficient—Application in computations of natural oil dispersion. *Proceedings,* 17th Arctic Marine Oil Spill Program Technical Seminar, Vancouver, BC, Canada, June 8–10. Emergencies Science Division, Environment Canada, Ottawa, ON, pp 173–187.
88. Coastal Engineering Research Center. 1984. *Shore Protection Manual,* Vol 1—Coastal Engineering Research Center, Department of the Army, Waterways Experiment Station, U.S. Army Corps of Engineers, Vicksburg, MS.
89. Lunel T. 1993. Dispersion: Oil droplet size measurements at sea. *Proceedings,* 16th Arctic Marine Oil Spill Program Technical Seminar, Calgary, AB, June 7–9. Emergencies Science Division, Environment Canada, Ottawa, ON, pp 1023–1056.
90. Hines AL, Maddox RN. 1985. *Mass Transfer Fundamentals and Application.* Prentice-Hall, Englewood Cliffs, NJ, USA.
91. Lyman CJ, Reehl WF, Rosenblatt DH. 1982. *Handbook of Chemical Property Estimation Methods.* McGraw-Hill Book, New York, NY, USA.
92. Di Toro DM, Zarba CS, Hansen DJ, Berry WJ, Swartz RC, Cowan CE, Pavlou SP, Allen HE, Thomas NA, Paquin PR. 1991. Annual review: Technical basis for establishing sediment quality criteria for nonionic organic chemicals using equilibrium partitioning. *Environ Toxicol Chem* 10:1541–1583.
93. French DP, Rines H. 1997. Validation and use of spill impact modeling for impact assessment. *Proceedings,* 1997 International Oil Spill Conference, Fort Lauderdale, FL, USA, April 7–10. API Publication 4651. American Petroleum Institute, Washington, DC, pp 829–834.
94. Craddock DR. 1977. Acute toxic effects of petroleum on arctic and subarctic marine organisms. In Malins DC, ed, *Effects of Petroleum on Arctic and Subarctic Marine Environments and Organisms,* Vol 2, Biological Effects. Academic, New York, NY, USA, pp 1–93.
95. Sprague JB. 1970. Measurement of pollutant toxicity to fish. II. Utilizing and applying bioassay results. *Water Res* 4:3–32.
96. Kooijman SALM. 1981. Parametric analysis of mortality rates in bioassays. *Water Res* 15:107–119.
97. French DP, French FW III. 1989. The biological component of the CERCLA type—A Damage Assessment Model system. *Oil Chem Pollut* 5:125–163.
98. McCarty LS, Ozburn GW, Smith AD, Bharath A, Orr D, Dixon DG. 1989. Hypothesis formulation and testing in aquatic bioassays: A deterministic model approach. *Hydrobiologia* 188/189:533–542.
99. McCarty LS, Mackay D, Smith AD, Ozburn GW, Dixon DG. 1992. Residue-based interpretation of toxicity and bioconcentration QSARs from aquatic bioassays: Neutral narcotic organics. *Environ Toxicol Chem* 11:917–930.
100. McCarty LS, Mackay D, Smith AD, Ozburn GW, Dixon DG. 1992. Toxicokinetic modeling of mixtures of organic chemicals. *Environ Toxicol Chem* 11:1037–1047.
101. Mackay D, Puig H, McCarty LS. 1992. An equation describing the time course and variability in uptake and toxicity of narcotic chemicals to fish. *Environ Toxicol Chem* 11:941–951.
102. Buikema AL Jr, Neiderlehner BR, Cairns J Jr. 1982. Biological monitoring. Part IV—Toxicity testing. *Water Res* 16:239–262.
103. Durbin AG, Durbin EG, Verity PG, Smayda TJ. 1981. Voluntary swimming speeds and respiration rates of a filter-feeding planktivore, the Atlantic Menhaden, *Brevoortia tyrannus* (Pisces: Clupeidae). *Fish Bull* 78:877–886.
104. Odum EP. 1971. *Fundamentals of Ecology.* W.B. Saunders, Philadelphia, PA, USA.
105. Di Toro DM, McGrath JA, Hansen DJ. 2000. Technical basis for narcotic chemicals and polycyclic aromatic hydrocarbon criteria. I. Water and tissue. *Environ Toxicol Chem* 19:1951–1970.
106. Di Toro DM, McGrath JA. 2000. Technical basis for narcotic chemicals and polycyclic aromatic hydrocarbon criteria. II. Mixtures and sediments. *Environ Toxicol Chem* 19:1971–1982.
107. Nirmalakhandan N, Speece RE. 1988. Structure–activity relationships, quantitative techniques for predicting the behavior of chemicals in the ecosystem. *Environ Sci Technol* 22:606–615.
108. Hodson PV, Dixon DG, Kaiser KLE. 1988. Estimating the acute toxicity of waterborne chemicals in trout from measurements of median lethal dose and the octanol–water partition coefficient. *Environ Toxicol Chem* 7:443–454.
109. Blum DJ, Speece RE. 1990. Determining chemical toxicity to aquatic species. *Environ Sci Technol* 24:284–293.
110. McCarty LS. 1986. The relationship between aquatic toxicity QSARs and bioconcentration for some organic chemicals. *Environ Toxicol Chem* 5:1071–1080.
111. McCarty LS, Mackay D. 1993. Enhancing ecotoxicological modeling and assessment. *Environ Sci Technol* 27:1719–1728.
112. Varhaar HJM, VanLeeuwen CJ, Hermens JLM. 1992. Classifying environmental pollutants, 1: Structure–activity relation-

ships for prediction of aquatic toxicity. *Chemosphere* 25:471–491.
113. Swartz RC, Schults DW, Ozretich RJ, Lamberson JO, Cole FA, DeWitt TH, Redmond MS, Ferraro SP. 1995. ΣPAH: A model to predict the toxicity of polynuclear aromatic hydrocarbon mixtures in field-collected sediments. *Environ Toxicol Chem* 14: 1977–1987.
114. Exxon Valdez Oil Spill Trustee Council. 1989. State/federal natural resource damage assessment plan for the *Exxon Valdez* Oil Spill, August 1989. Public Review Draft. *Exxon Valdez* Oil Spill Trustee Council, Juneau, AK, USA.
115. Galt JA, Lehr WJ, Payton DL. 1991. Fate and transport of the *Exxon Valdez* oil spill, Part 4 of a five-part series. *Environ Sci Technol* 25:202–209.
116. Payne JR, Clayton JR Jr, Daniel McNabb G Jr, Kirstein BE. 1991. *Exxon Valdez* oil weathering fate and behavior: Model predictions and field observations. *Proceedings,* 1991 International Oil Spill Conference, San Diego, CA, USA, March 4–7, American Petroleum Institute, Washington, DC, pp 641–654.
117. Wolfe DA, Hameedi MJ, Michel J, Galt JA, Watabayashi G, Payne JR, Short J, O'Claire C, Rice S, Braddock J, Hanna S, Sale D. 1994. The fate of the oil spilled from the *Exxon Valdez*. *Environ Sci Technol* 28:561–568.
118. Gundlach E, Pavia EA, Robinson C, Civeaut JC. 1991. Shoreline surveys at the *Exxon Valdez* oil spill: The state of Alaska response. *Proceedings,* 1991 International Oil Spill Conference, San Diego, CA, USA, March 4–7, American Petroleum Institute, Washington, DC, pp 519–529.
119. Isaji T, Spaulding ML. 1987. A numerical model of the M2 and K2 tide in the northwestern Gulf of Alaska. *J Phys Oceanogr* 17:698–704.
120. Okubo A, Ozmidov RV. 1970. Empirical dependence of the coefficient of horizontal turbulent diffusion in the ocean on the scale of the phenomenon in question. *Atmospheric and Ocean Physic* 6:534–536.
121. Day RH, Murphy SM, Wiens JA, Hayward GD, Harner EJ, Smith LN. 1995. Use of oil-affected habitats by birds after the *Exxon Valdez* oil spill. In Wells PG, Butler JN, Hughes JS, eds, Exxon Valdez *Oil Spill: Fate and Effects in Alaskan Water*. STP 1219. American Society for Testing and Materials, Philadelphia, PA, pp 726–761.
122. Piatt JF, Lensink CJ, Butler W, Kendziorek M, Nysewander DR. 1990. Immediate impact of the *Exxon Valdez* oil spill on marine birds. *Auk* 107:387–397.
123. Ford RG, Bonnell ML, Varoujean DH, Page GW, Carter HR, Sharp BE, Heinemann D, Casey JL. 1996. Total direct mortality of seabirds from the *Exxon Valdez* oil spill. *Am Fish Soc Symp* 18:684–711.
124. Schempf PF, Bowman TD, Bernatowicz J. 1992. Assessing the effect of the *Exxon Valdez* oil spill on bald eagles. Bird Study 4. Annual Progress Report—1991. November 22, 1991, revised May 12. *Exxon Valdez*. Oil Spill Trustee Council, Juneau, AK, USA.
125. *Exxon Valdez* Oil Spill Trustee Council. 1991. Summary of the effects of the *Exxon Valdez* oil spill on natural resources and archaeological resources. Juneau, AK, USA, Filed by U.S Department of Justice, U.S. District Court, Alaska, Civil Action No. A91-082.
126. Neff JM, Burns WA. 1996. Estimation of polycyclic aromatic hydrocarbon concentrations in the water column based on tissue residues in mussels and salmon: An equilibrium partitioning approach. *Environ Toxicol Chem* 15:2240–2253.